Schweizerische Eidgenossenschaft
Confédération suisse
Confederazione Svizzera
Confederaziun svizra

Federal Department of the Environment, Transport, Energy and Communications DETEC

Swiss Federal Office of Energy SFOE
Energy Research and Cleantech

Final report

ImproCIS

Improving the energy efficiency of thin film CIGS solar cells and mini-modules

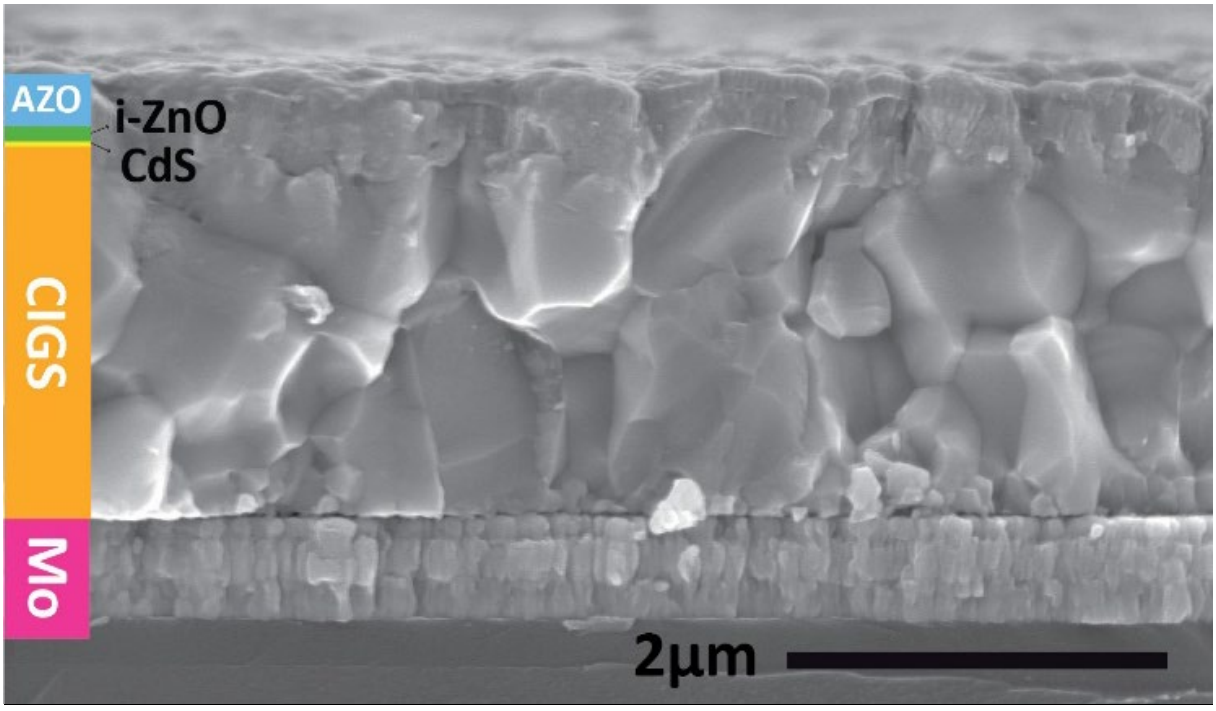

Source: ©Empa 2021

Empa
Materials Science and Technology

Date: 20.04.2021

Location: Bern

Publisher:
Swiss Federal Office of Energy SFOE
Energy Research and Cleantech
CH-3003 Bern
www.bfe.admin.ch

Co-financing:
Swiss Federal Office of Energy SFOE
Energy Research and Cleantech
CH-3003 Bern
www.bfe.admin.ch

Subsidy recipients:
Laboratory for Thin Films and Photovoltaics, Empa
Überlandstr. 129
CH-8600 Dübendorf
www.empa.ch

Authors:
S.-C. Yang, Empa, Laboratory for Thin Films and Photovoltaics, shih-chi.yang@empa.ch
R. Carron, Empa, Laboratory for Thin Films and Photovoltaics, romain.carron@empa.ch
A. N. Tiwari, Empa, Laboratory for Thin Films and Photovoltaics, ayodhya.tiwari@empa.ch

SFOE project coordinator:
Dr. Stefan Oberholzer, stefan.oberholzer@bfe.admin.ch

SFOE contract number: SI/501614-01

The authors bear the entire responsibility for the content of this report and for the conclusions drawn therefrom.

Zusammenfassung

Cu(In,Ga)Se2 (CIGS) -Dünnschichtsolarzellen werden aufgrund ihrer nachgewiesenen Vorzüge der hohen photovoltaischen (PV) Umwandlungs-Effizienz, der langfristigen Leistungsstabilität und ihrem Potential für kostengünstige Solarmodule aufgrund der inhärenten Vorteile der Dünnschichtherstellungstechnologien, die eine Produktion mit hohem Durchsatz auf großflächigen Substraten mit geringem Energieverbrauch - insbesondere per Rolle-zu-Rolle-Verfahren – als wichtig für die industrielle Produktion erachtet.

Ziel des Projekts war es, flexible CIGS-Solarzellen mit einem Wirkungsgrad von 22% mit einem Verfahren zu entwickeln, das für Folien - vorzugsweise Polymerfolie, ansonsten Metallfolie als alternative Ersatzstrategie, wobei die Kompatibilität der Abscheidungsprozesstemperatur mit industriellen Rolle-zu-Rolle-Verfahren berücksichtigt wird - geeignet ist In diesem Zusammenhang bestand die zentrale Herausforderung darin, zunächst zu verstehen, warum die Wirkungsgrade über 20% mit Folien schwer zu erreichen sind.

Wir untersuchten den Einfluss des Substrats (Glas, Stahl, Polyimid) und der Prozesstemperaturen und stellten fest, dass die Beschaffenheit des Substrats bei Niedertemperaturprozessen (~ 450°C, kompatibel mit Polyimidsubstraten) eine marginale Rolle spielt. Die Eigenschaften der CIGS-Schichten, die bei höheren Temperaturen auf Glassubstraten abgeschieden werden, sind anders und führen zu Solarzellen mit höherem Wirkungsgrad. Durch Erhöhen der Abscheidungstemperatur auf >550°C konnten wir einen absoluten Wirkungsgradgewinn von 1% (von 20.4% auf 21.5%) erzielen. Aufgrund unserer Präferenz für Polyimidsubstrat haben wir jedoch unsere Bemühungen zur Verbesserung der Eigenschaften von bei niedrigereren Temperaturen abgeschiedenen CIGS-Schichten durch Modifizierung des Wachstumsprozesses priorisiert, insbesondere durch Optimierung der Methode zur Inkorporation von Alkali in CIGS und der Gradienten der elementaren Zusammensetzung.

Mit verbesserten Methoden zur Inkorporation von Alkali konnten wir zwei aufeinanderfolgende Effizienzverbesserungen nachweisen, die in einer Solarzelle auf einem flexiblen Polyimidsubstrat mit einer zertifizierten Effizienz von 21.38% resultierte. Wir haben einen vielversprechenden Weg für weitere Effizienzgewinne durch das Legieren mit Silber identifiziert, der neue Möglichkeiten für hocheffiziente Solarzellen bei deutlich verringerten Abscheidungstemperaturen eröffnet.

Um den Wirkungsgradverlust von Zelle zu Modul zu verringern, haben wir eine detaillierte Untersuchung der optischen und elektrischen Verluste in der Gerätestruktur und der parasitären Shunts durchgeführt, die sich während den Laserablationsschritten entwickeln. Wir konnten einen Wirkungsgradverlust von Zelle zu Modul von 2.1% für gelaserte Minimodule erzielen, die auf einem flexiblen Polyimidfilm hergestellt wurden. Die Ergebnisse legen nahe, dass verbleibende Füllfaktorverluste insbesondere durch eine weitere Untersuchung des Potenzials von blauen Lasern als Ablationswerkzeug gemindert werden können.

Résumé

Les cellules solaires à couches minces Cu(In,Ga)Se_2 (CIGS) sont considérées comme importantes en raison de leurs mérites éprouvés pour une efficacité de conversion photovoltaïque (PV) élevée, une stabilité des performances à long terme et un potentiel pour des modules solaires à faible coût. Les avantages inhérents aux technologies de fabrication de couches minces permettent une production à haute vitesse et de faible consommation d'énergie sur des substrats de grande surface, en particulier par des méthodes de production industrielle rouleau-à-rouleau.

L'ambition du projet était de développer des cellules solaires CIGS flexibles avec une efficacité de 22% avec un procédé adapté aux feuilles - de préférence un film polymère, sinon avec une feuille métallique comme stratégie alternative de repli, en gardant à l'esprit la compatibilité en température du processus de dépôt industriel rouleau-à-rouleau. Dans ce contexte, le principal défi était de comprendre d'abord pourquoi les rendements au-delà de 20% sont difficiles à atteindre avec les feuilles.

Nous avons étudié l'influence du substrat (verre, acier, polyimide) et des températures de déposition, et avons constaté que la nature du substrat joue un rôle marginal pour les processus à basse température (~450°C compatible avec les substrats en polyimide). Les propriétés des couches de CIGS déposées à des températures plus élevées sur des substrats en verre sont différentes et conduisent à des cellules solaires plus efficaces. Nous pourrions atteindre un gain d'efficacité de 1% absolu (de 20.4% à 21.5%) en augmentant la température de dépôt à >550°C. Cependant, en raison de notre préférence pour les substrats en polyimide, nous avons priorisé nos efforts pour améliorer les propriétés des couches de CIGS déposées à basse température en modifiant le processus de croissance, notamment en optimisant la méthode d'incorporation d'alcali dans le CIGS et les gradients de composition d'éléments.

Grâce à des méthodes améliorées d'incorporation d'alcali, nous avons démontré deux améliorations successives du record d'efficacité, aboutissant à une cellule solaire certifiée à 21.38% sur un substrat flexible en polyimide. Nous avons identifié une voie prometteuse pour des gains d'efficacité supplémentaires grâce à l'alliage d'argent qui ouvre de nouvelles voies pour les cellules solaires à haut rendement à une température de dépôt beaucoup plus basse.

Pour réduire la perte d'efficacité cellule à module, nous avons effectué une enquête détaillée sur les pertes optiques et électriques dans la structure de modules et les shunts parasites qui se développent au cours des étapes de marquage laser. Nous avons obtenu une perte d'efficacité cellule à module de 2,1% pour les mini-modules gravés au laser fabriqués sur un film polyimide flexible. Les résultats suggèrent que les pertes de fill factor restantes peuvent être atténuées notamment en explorant plus avant le potentiel du laser bleu en tant qu'outil de marquage.

Summary

Cu(In,Ga)Se_2 (CIGS) thin film solar cells are considered important because of their proven merits for high photovoltaic (PV) conversion efficiency, long-term performance stability, and potential for low-cost solar modules. The inherent advantages of thin film manufacturing technologies enable high throughput production on large area substrates with low energy consumption, especially with roll-to-roll methods for industrial production.

The ambition of the project was to develop flexible CIGS solar cells with an efficiency of 22% with a process suitable for foils- preferably polymer film, otherwise with metal foil as a fall-back alternative strategy, keeping in mind the deposition process temperature compatibility with roll-to-roll industrial manufacturing. In this context, the key challenge was to first understand why the efficiencies beyond 20% are difficult to reach with foils.

We investigated the influence of substrate (glass, steel, polyimide) and process temperatures and found that the nature of the substrate plays a marginal role for low-temperature processes (~450°C compatible with polyimide substrates). The properties of the CIGS layers deposited at higher temperatures on glass substrates are different and lead to higher efficiency solar cells. We could achieve an efficiency gain of 1% absolute (from 20.4% to 21.5%) by increasing the deposition temperature to >550 °C. However, because of our preference for polyimide substrate we prioritized our efforts to improve the properties of low-temperature deposited CIGS layers by modifying the growth process, especially by optimizing the alkali incorporation method in CIGS and elemental composition gradients.

With improved alkali incorporation methods, we demonstrated two successive efficiency record improvements, culminating in a 21.38% certified solar cell on a flexible polyimide substrate. We identified a promising path for further efficiency gains by silver alloying which opens new pathways for high-efficiency solar cells at much lower deposition temperature.

To reduce the cell-to-module efficiency loss we performed a detailed investigation of optical and electrical losses in device structure and parasitic shunts which develop during the laser scribing steps. We could achieve a cell-to-module efficiency loss of 2.1% for laser scribed mini-modules fabricated on flexible polyimide film. Results suggest that remaining fill factor losses can be mitigated notably by exploring further the potential of blue laser as scribing tool.

Main findings

Our main findings are summarized as follows:

- For CIGS solar cell technology, the choice of the substrate (glass, steel, polyimide) has a minor impact at low processing temperatures compatible with flexible polyimide substrates. By contrast, the choice of the substrate plays an important role with processes at higher temperatures.
- Improved deposition processes were developed to improve the quality of the absorber layers, improving the record power conversion efficiency for flexible CIGS cells on polymer foils from 20.4% to 21.4%.
- Modified module interconnection laser patterning and passivation layer processes were developed to suit the device structure with improved absorbers, enabling low 2.1% cell-to-module efficiency loss.
- The improved processes and knowledge can be made available to the company Flisom AG for improvement of performance and competitiveness of their roll-to-roll manufacturing of flexible solar modules. Lightweight flexible solar modules are attractive for applications on buildings and transport vehicles - to reduce the CO_2 emission and hence contributing towards enhanced sustainability, which is much needed for Switzerland's green energy policy.

Contents

Abbreviations

List of used abbreviations

ACIGS	(Ag,Cu)(In,Ga)Se_2 semiconductor
ALD	Atomic layer deposition
CGI	[Cu] / ([Ga] + [In]) composition ratio
CIGS	Cu(In,Ga)Se_2 semiconductor
C-V	Capacitance versus voltage
CVD	Chemical vapor deposition
FF	Fill factor
GGI	[Ga] / ([Ga] + [In]) composition ratio
HLS	Heat-light soaking
J_{SC}	Short-circuit current
J-V	Current density versus voltage
PCE	Power conversion efficiency
PDT	Post deposition treatment
PI	Polyimide
PL	Photoluminescence
PV	Photovoltaic
SEM	Scanning electron microscope
SIMS	Secondary ion mass spectroscopy
SLG	Soda-lime glass
TCO	transparent conductive oxide
TRPL	Time-resolved photoluminescence
UV	Ultraviolet
V_{OC}	Open-circuit voltage
WP	Work package
XRD	X-ray diffraction
ΔGGI	Height of the Ga back gradient (definition in section 3.3.3)

1 Introduction

1.1 Background information and current situation

$Cu(In,Ga)Se_2$ (CIGS) thin film solar cells are considered important because of their proven merits for high photovoltaic (PV) conversion efficiency, long term performance stability and potential for low-cost solar modules due to the inherent advantages of thin film manufacturing technologies enabling high throughput production on large area substrates with low energy consumption.

Si wafer-based modules, mostly produced in China, currently have a market share of 95% but these modules are rigid and heavy. Similarly, state-of-the-art thin film modules on the market based on CdTe (First Solar) and CIGS (e.g. Solar Frontier K.K, NICE solar Energy, Avancis) are also rigid and heavy.

There is a lack of flexible and lightweight solar modules while there are numerous applications, with huge market potential, where conventional (rigid and heavy) solar modules are either not applicable or have certain limitations. In this context, the development of flexible solar modules with high photovoltaic conversion efficiency and long-term stable performance is important. The market share of flexible and lightweight thin film PV is bound to grow, provided the challenges related to production of high-efficiency modules with high throughput and yield could be managed in a cost-effectively. Flexible CIGS modules can be manufactured on polymer foils with reduced deposition temperatures, or alternatively on heavier and more expensive steel foils. Our lab has specialized in the development of CIGS thin film solar cells on polymer substrates with low-temperature processes. Such a process developed at Empa provides the underlying concepts for adaptation to roll-to-roll manufacturing by Flisom AG for commercialization of lightweight flexible solar modules for different applications globally.

The CIGS technology has progressed remarkably in recent years and the highest record conversion efficiencies of 22.6% on glass substrates with high temperature (>550 °C) and 20.4% on polymer film with low temperature (~450 °C) CIGS deposition methods were achieved by research labs at ZSW and Empa, respectively. By the end of the project, the record efficiencies have been pushed to 23.35 (high temperature, Solar Frontier K. K.) and thanks to this project, to 21.38% for low temperature by Empa.

Swedish company Midsummer produces CIGS solar cells on stainless steel (wafer size of about 15x15 cm^2) and interconnects these individual cells to assemble into modules - similar to Si wafer technology. However, stainless steel with high diffusion barrier coatings and smooth surface should be rather expensive and significantly heavier than polyimide (PI) film.

Last year, the Korean Institute of Energy Research (KIER) announced a 20.4% efficiency flexible CIGS thin film solar cell on polyimide film developed with a process similar to Empa. Meanwhile, Empa made further progress to a new record efficiency of 21.4% achieved recently with the support of ImproCIS project.

1.2 Purpose of the project

The ImproCIS project was planned to understand the differences in the properties of low and high temperature grown CIGS layers and solar cells, and then implement the new learnings to further increase the efficiency of flexible solar cells beyond the current state-of-the-art values.

Retrospectively, the ambition of the lab was to develop more than 22% flexible CIGS solar cells with a process suitable for foils - preferably polymer film and otherwise with metal foil as a fallback alternative strategy. In this context, the key challenge is to first understand why we are unable to achieve cell efficiencies beyond 20%: is it the low-temperature CIGS process of Empa? How and what properties of CIGS grown at high temperature (> 550°C) are different and what type of recombination loss has been limiting our flexible solar cells? As such, incremental enhancement of efficiency from a high level of

reference value becomes a very tedious task. While one can improve on one PV parameter (e.g. current) but then either fill factor or the voltage might drop. So, the processing challenge is to increase all three photovoltaic parameters or at least not degrade one at the cost of the other. Unfortunately, as far as the current state of the art of flexible CIGS is concerned there is no one isolated challenge or key issue which can be pointed out except for the bulk qualities of CIGS layers and interfaces. Linked to this are the roles of substrates and impurities from substrates.

The successfully concluded project was planned to take a step back from the state of the art process used at the beginning of the project: we wanted to understand the differences in the properties of low and high temperature grown CIGS layers and solar cells and then implement the knowledge to further increase the efficiency of flexible solar cells beyond those current state of the art values. The targets were:

I. Increase the highest efficiency of flexible solar cells to values similar to that achieved on glass substrates.

II. Establish the roles of different substrates (glass, polyimide, metal) on properties of CIGS layers and achievable highest cell efficiencies on respective substrates.

III. A robust CIGS process which consistently delivers high efficiencies with narrow distribution with respect to fluctuations in deposition conditions (broad processing window is desired by industries)

1.3 Objectives

This section recapitulates the project proposal to provide context for the results achieved during the ImproCIS project.

The anticipated efficiency related results are:

I. Flexible solar cells with efficiency >22%.

II. Identification of flexible substrates with or without barrier layers to consistently deliver cell efficiencies >21.5%.

III. Mini-modules with efficiencies >18% (with support from Flisom on interconnects).

2 Procedures and methodology

Three work packages (WP) were defined to achieve key deliverables in 3 years project duration:

WP1 - Solar cells on glass substrates: The typical device efficiency increase with higher deposition temperatures, and the goal of the WP1 is to understand the key differences between low and high deposition processes, especially in terms of the dependence of electronic properties and morphologies on composition (concentration ratios of different elements and their depth profiles. The WP is subdivided into 4 tasks. (a) Integration of a metal flux measurement tool, to improve the control on layer manufacturing by in-situ control of relative rates during the co-evaporation process. (b) Evaluation of suitable glass including barrier/buffer layer. (c) Detailed comparison of low and high temperature processed solar cells, and (d) Explore efficiency limits of CIGS solar cells on glass. The results are reported in section 3.1.

WP2 - Flexible solar cells on metal foils: Owing to their compatibility with high processing temperatures, steel foils may be considered as an alternative to polymer foils for flexible photovoltaic applications, despite their high cost and lesser flexibility. The WP is divided into two aspects. (a) Evaluation of suitable metal foils including barrier/buffer layer. (b) Benchmarking of processes and effects of deposition temperature identified for possible adaptation on polymer at low temperature. The results are presented in section 3.2, together with aspects of the analysis of high-temperature glass samples.

WP3 - Flexible solar cells and mini-modules on polyimide foils: The challenges are addressed in 3 tasks. (a) Explore ultraviolet (UV) flash annealing of CIGS on different substrates (section 3.3.1). (b) Explore efficiency limit of CIGS solar cells on polymer film. We took into account the knowledge acquired in WP1 and WP2, and we also developed new approaches to overcome the challenges encountered. The results are presented in sections 3.3.2 - 3.3.6. (c) Explore efficiency limit of CIGS solar modules on polymer film, by realization of mini-modules (section 3.3.7).

Figure 1 presents the typical device structure of a CIGS solar cell. The total thickness of the active layers is about 3 µm, in addition to the substrate itself which is 10 to 50 µm thick in the case of polyimide foils.

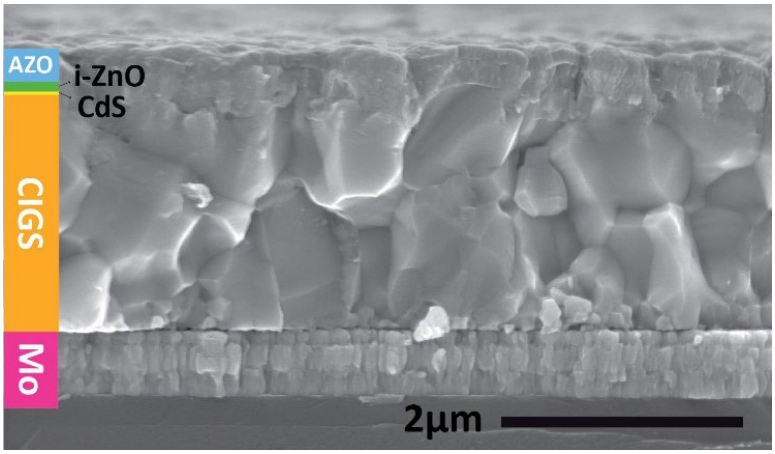

Figure 1: Typical device structure of a CIGS solar cell. From bottom to top: substrate (glass, polyimide or steel), Mo back contact, bandgap-graded CIGS, CdS and ZnO buffer layers, and ZnO:Al (AZO) transparent conductive oxide (TCO). Figure adapted from [1]

3 Results and discussion

3.1 WP 1 Solar cells on glass substrates

The activity of WP1 ended in 2019. In addition to the results reported below, an in-depth analysis of charge transport and recombination was conducted and is summarized in the section WP2.

3.1.1 Metal flux measurement system

High-quality absorber layers are grown with graded bandgap by changing the metal flux ratios. In-situ, real-time measurement of metallic fluxes in CIGS deposition tools would be an important asset for knowledge-based process development. In April 2018, we installed in our CIGS deposition system an in-situ sensor for the metal fluxes, based on a quadrupole mass spectrometer (QMS) sensor.

After facing initial difficulties with the tool sensitivity, two extensive testing sessions were organized with the tool manufacturer to characterize the tool performance with different hardware configurations. The system is capable of real-time monitoring the Se flux, a capability however not needed in our system thanks to our inline Se beam laser flux monitoring. The equipment was found unsuitable for measuring the fluxes of metals (Cu, In, Ga) in our system in operating conditions.

The tool presents three major shortcomings:

1. The signal to noise ratio is too low (by about 2 orders of magnitude) to use in processing conditions
2. Drift of the zero-level signal over time.
3. Slow response of the detection chain to changes in machine conditions (shutter, etc.), in the range of 2-3 minutes.

Despite adaptations of the system suggested by the manufacturer (e.g. installation of a by-pass pump system), these issues could only be marginally improved and performance remained far from the expected levels. Finally, the metal flux monitor system was unmounted from the CIGS evaporator.

3.1.2 Evaluation of new glass substrate

Different types of glasses - in terms of thermal expansion coefficients, alkali composition, and thickness were evaluated for their compatibility with our existing deposition equipment and processing temperatures (e.g. the softening point of glass depends on its composition). Glass substrates with and without barrier layers were investigated, to inhibit the alkali diffusion from the glass during the CIGS growth. We could achieve good results, as reported in the following section. This knowledge is essential to understand the influence of alkali when available or absent during the growth of CIGS layers. The polymer substrates aimed in this project (WP3) do not contain such alkali elements.

3.1.3 High temperature processing and efficiency limits

Our hypotheses for limited device performance at low temperature are non-uniformities on the micrometer scale in lateral distribution of matrix elements, and the presence of voids of several hundred nanometers below the CIGS surface. They are expected to change if the substrate temperature is increased. To prove those hypotheses, in May 2018 we installed a new characterization tool allowing the measurement of the lateral distribution of recombination properties with micrometer resolution by time-resolved photoluminescence (TRPL). The related results are briefly presented in Section 3.2 together with the results on metal foils.

With suitable high-temperature glass evaluated in Section 3.1.2, the efficiency of CIGS solar cell could reach 21.5% after application of an anti-reflection coating. This is about 1% higher than the corresponding devices grown at low temperatures. The improvement in efficiency is attributed to a longer lifetime and larger grain size as evidenced by TRPL and scanning electron microscope (SEM) cross-section, which reduces the activity of the non-radiative recombination channels. The TRPL decays are extended about 2-fold, which corresponds to an increase in the quasi-Fermi level for electrons by about 20 meV. This value matches very well the improvement observed in the deficit of open-circuit voltage (V_{OC}). In addition, a slight improvement in the fill factor of about 1% was also observed.

The performances of the absorbers deposited at high temperatures fabricated within this project remained below the state-of-the-art. The short-circuit current corresponds to the expectations, and could be slightly improved by careful optimization of the bandgap gradient as well as the implementation of advanced light management strategies. An example of such a strategy is the use of advanced anti-reflection foils, a technique suitable at laboratory scale but that cannot be transferred to industrial partners. The fill factor of the high-temperature cells is slightly improved as compared to low-temperature devices. The reason for it is not well understood and deserves further investigation. Last, the open-circuit voltage slightly improves following a reduction of the activity of the non-radiative recombination channels. We attribute the efficiency loss of our low-temperature process to about 1%.

3.2 WP2 Flexible solar cells on metal foils

3.2.1 Evaluation of suitable metal foil including barrier/buffer layer

Based on initial evaluation results, we chose SS340 foils as a metal substrate that presents a good compromise in terms of coefficient of expansion mismatch with CIGS, melting point and density. The thickness of the stainless steel substrate is around 30µm. Figure 2 shows the appearance of the metal substrate as well as the image taken under optical microscopy. Relatively smooth surfaces were observed.

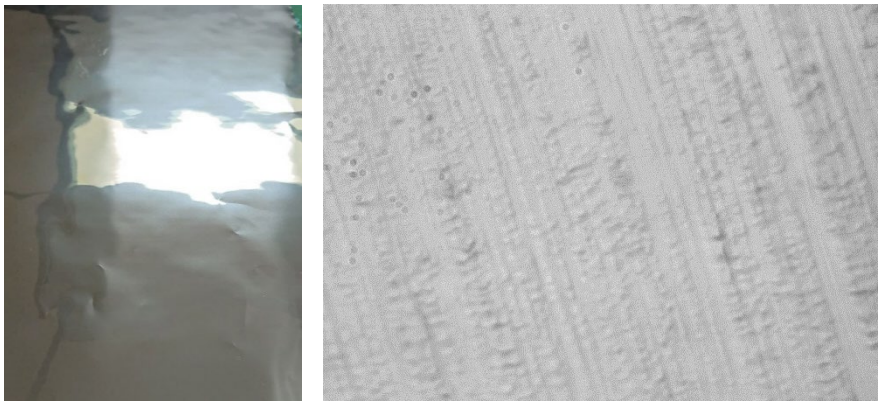

Figure 2: The appearance of SS340 metal (stainless steel) substrate (reflection of the ceiling lamp), and optical microscopy image.

3.2.2 Benchmarking of processes and effects of deposition temperature identified for possible adaption on polymer at low temperature

CIGS solar cells were grown on metal foils using both high and low deposition temperatures. Different barrier layers were also evaluated to understand the effects of diffusion of impurities from the substrates.

For low-temperature processes, the efficiencies were slightly degraded as compared to the reference glass substrates, driven by a slight decrease in the V_{OC}. The presence of a barrier to prevent the diffusion

of impurities from the substrate was found to have a small, but inconsistent effect. The other properties of the absorbers were found quite similar to the reference glass sample, in terms of morphology, grain size, as well as the concentration of Ga and In as functions of the depth in the absorber. Our low-temperature processes lead to comparable properties of absorbers on metal, glass and PI, in terms of morphology, composition, and doping level.

Solar cells with good performances were obtained with high-temperature processes, attested by a 20.15% independently certified cell. Our value is only slightly short of the record value of 20.56% [2], obtained on expensive stainless foil coated with an impurity diffusion barrier layer and using sputtering for absorber deposition at a high substrate temperature. The absorber properties deviate significantly in case of higher deposition temperatures, especially in terms of compositional gradients and doping densities. The reasons for the extremely low V_{OC} deficits of steel samples (indicative of good semiconductor and device with low non-radiative loss to yield high efficiency) were investigated further and findings are presented in the section below. The lower bandgap obtained with this process is also interesting in view of tandem device applications, thanks to the improved conversion of near-infrared photons. Two publications are in preparation to discuss the differences between glass and metal substrates and the impact of lateral inhomogeneities on device performances.

In the following, we report the detailed analysis of the performances and the charge transport in the absorber layer, based on photoluminescence (PL) and TRPL mapping as main investigation tools.We investigated the following samples:

- SLG (LT) no PDT: an absorber processed at low temperature on soda-lime glass (SLG) substrate with barrier layer, without any alkali post-deposition treatment (PDT). As expected, this device performs significantly worst that the other ones.
- SLG (LT) NaF: an absorber processed on SLG substrate at low temperature with NaF PDT.
- SLG (LT) NaF+RbF: similar to the former, additionally treated with RbF PDT for higher efficiency > 20%. This sample is representative of our baseline with PI substrate.
- SLG (HT) NaF+RbF: deposited at high temperature, with efficiency > 21%.
- Steel (HT) NaF+RbF: deposited at high temperature on stainless steel substrate, with device efficiency of 20%.

PL and TRPL were used to learn the fundamental electronic properties of the absorber layer and predict device performance and such measurements can be performed before device completion (e.g. on bare absorbers or after CdS buffer deposition). Both techniques can be implemented as quality control in a manufacturing line to obtain almost real-time information on the deposition process. As compared to PL, TRPL offers additional advantages. First, from the signal peak intensity A values immediately after pulsed laser excitation, one can discriminate issues related to doping levels typically related to the alkali doping process. Second, issues with non-radiative recombination lifetime τ (characteristic signal decay time after illumination) comparatively suggest issues with CIGS matrix elements Cu, In, Ga and Se. Figure 3a compares the predictions of V_{OC} obtained with PL and TRPL. Both techniques are effective to predict the device experimental V_{OC} (stars). As compared to PL, TRPL provides an additional level of information (Figure 3b) and discriminates between issues related to absorber doping and from non-radiative recombination, from which targeted feedback to the manufacturing line can be obtained. As an example, absorbers on steel and high-temperature glass show excellent V_{OC}, which originate from very different combinations of non-radiative recombination and doping levels in the absorbers. In WP3 we developed an alternative method to increase the doping level in the absorbers grown at low temperature on PI substrates.

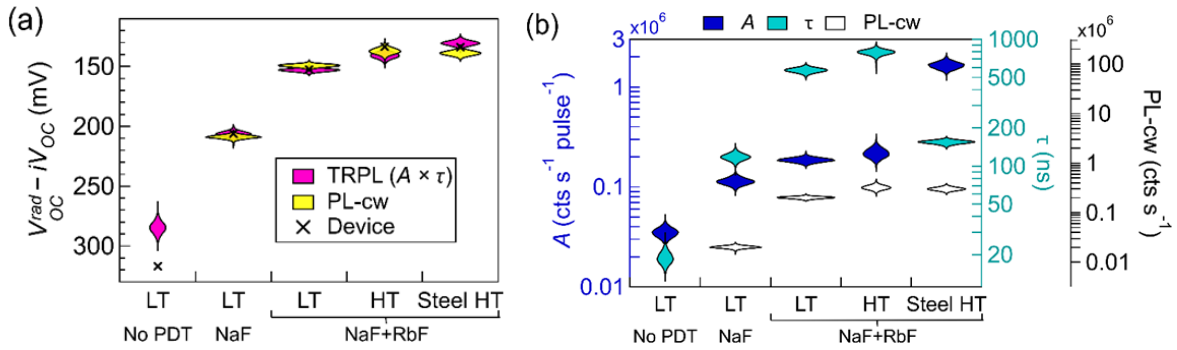

Figure 3: (a) Non-radiative VOC deficit calculated for two different figure of merits: PL, and A × τ from TRPL. Black crosses use the device VOC for the calculation of non-radiative voltage loss. (b) Distribution of TRPL parameters A, τ, and integrated steady state PL at equivalent one-sun illumination intensity. The distribution stem from scanning PL and TRPL data. Both PL and TRPL predict well the device VOC. TRPL provides additional information (doping level, recombination) from which targeted feedback to the manufacturing line can be obtained.

We also conducted an in-depth analysis of the transport of electrical charge carriers in the same series of absorbers. The samples were characterized by TRPL mapping and the experimental data were confronted to numerical simulations. The results are displayed in Figure 4 both graphically and as a summary table. The steel substrate leads to inferior mobility and diffusion length of charge carriers. The mobility values are sufficiently low to become an issue, possibly limiting the photovoltaic performances of samples on steel substrates.

Comparison of the samples on glass substrates reveals that the high-temperature process improves the layers in terms of non-radiative recombination level, leading to the observed improved performances. The diffusion length of charge carriers is correspondingly improved because of the lower recombination. The grain boundaries and the PDT treatments affect the charge carrier recombination but are appear benign in terms of diffusion and scattering of charge carriers. For the absorbers grown on glass substrates, the mobility value determined is sufficiently large and is not a limiting factor to the device performance with the usual device architecture. A publication in preparation will present the results in detail.

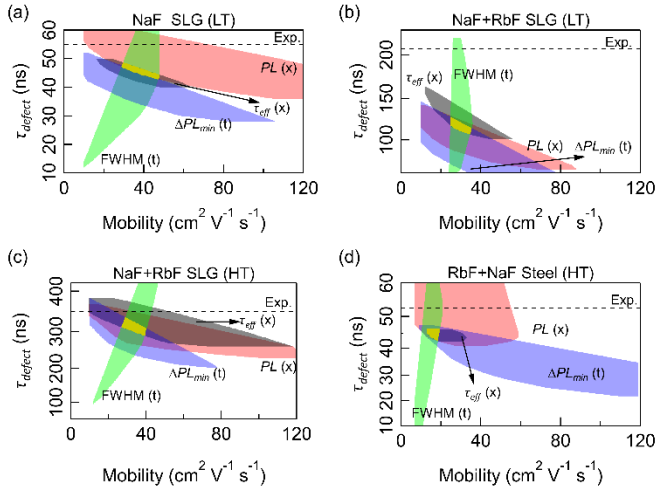

Sample	PDT	μ ($cm^2V^{-1}s^{-1}$)	τ_{eff} (ns)	L_D (μm)
SLG (LT)	NaF	26 to 50	105	2.7 to 3.7
SLG (LT)	NaF+RbF	23 to 37	570	5.8 to 7.4
SLG (HT)	NaF+RbF	25 to 42	780	7.1 to 9.2
Steel	NaF+RbF	9 to 21	155	1.9 to 2.9

Figure 4: (left) Evaluation of the parameter space (τ_{defect} and mobility) for absorbers processed on different substrates and under different conditions. Shaded regions correspond to accepted fits of the different data analysis methods. The gold region corresponds to the intersection region of the analysis methods, leading to the range of accepted parameter values presented in the table (right). The low mobility value found for the sample on steel may be limiting the device performance.

3.3 WP3 Flexible solar cells and mini-modules on polyimide foils

In WP3 we explored different strategies to improve the cell performances. We investigated the treatment of devices with UV flash annealing. We improved the CIGS deposition processes with innovative alkali incorporation strategies, and we quantified the impact on the performances of non-optimal absorber composition gradients. With heat-light soaking treatment, we developed an alternative strategy to increase the doping level in the absorber and match the high values demonstrated in WP2 on steel substrates. We identified alloying with Ag as the most promising strategy for the next efficiency progresses especially regarding low-temperature processing.

We finally report our efforts to ensure compatibility of the improved absorber deposition processes with module manufacturing through mini-module making.

3.3.1 Explore UV flash annealing of CIGS absorbers

The UV flash annealing was used to locally anneal the CIGS without excessive heating of the substrate. However, no improvements were found at different power densities. On the contrary, a drop in cell efficiency was observed when the voltage for the UV flash lamp was higher than a threshold value (Figure 5).

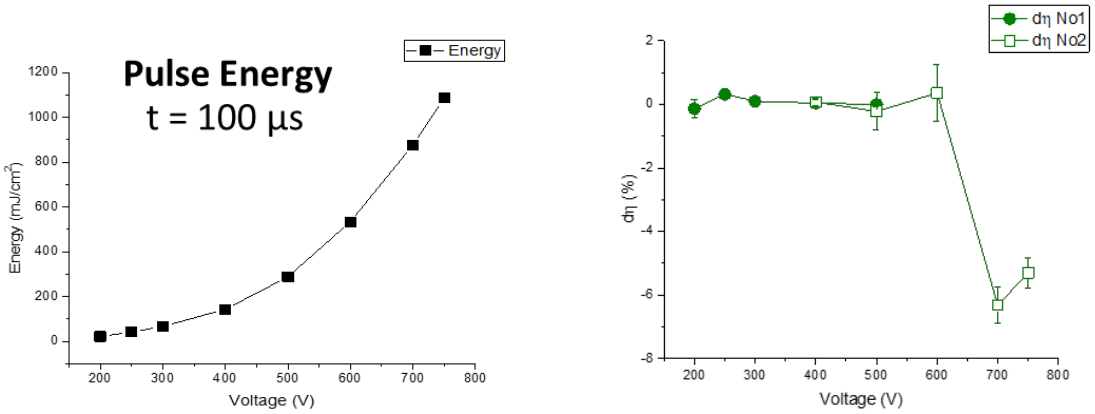

Figure 5: (a) Energy density versus input voltage in UV flash annealing. (b) The change in efficiency of 2 different cells after UV flash annealing with different pulse energy.

We conclude that the heating of the absorber is not able to improve the photovoltaic performances of our CIGS cells. Possible reasons could be that the UV annealing does not affect the CIGS layer in a selective enough manner, and the buffer and top electrode are damaged by the treatment. Our current equipment does not allow for more selective layer annealing.

3.3.2 Improved CIGS deposition process

Different strategies for incorporating alkali elements into CIGS were evaluated based on a large number of depositions. Figure 6(left) shows the deposition sequence for different process variants (A-D). Figure 6(right) reports the sample power conversion efficiency for the four technological steps investigated in the study. The efficiency of each sample corresponds to the average of up to 18 individual cells measured without antireflection coating.

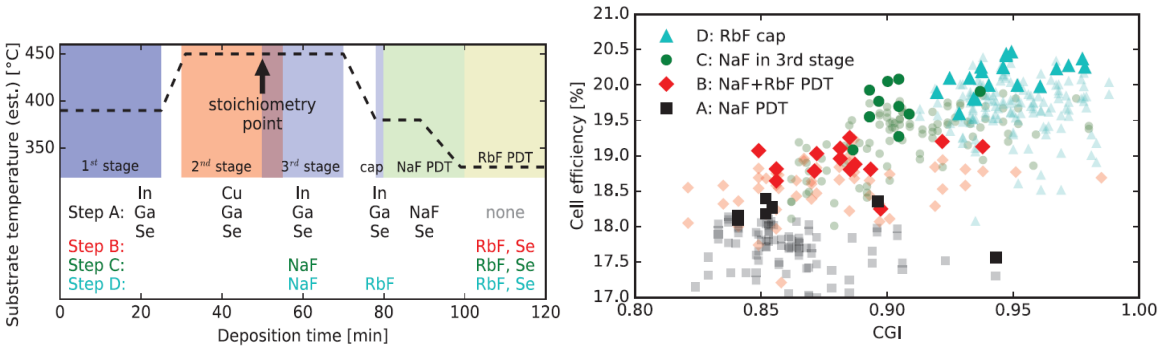

Figure 6: (left) Typical CIGS deposition sequences of the baseline process A (black), as well as technological steps B (red), C (green), and D (cyan). The dashed line indicates the estimated actual substrate temperature. (right) Cells efficiency as function of the absorber Cu content CGI ([Cu]/([Ga]+[In])), for the four investigated technological steps (without anti-reflective coating). Small symbols refer to sample averages (up to 18 cells). The large symbols show individual cells. The improved manufacturing processes with modified absorber composition enable higher cells efficiencies.

Implementing the improved deposition process D and after deposition of a MgF_2 antireflection coating, a champion device on PI substrate was independently certified, yielding a record for CIGS on flexible substrate with 20.8% power conversion efficiency. The photovoltaic parameters of this cell are reported in Table 2. The results and the record cell are presented in detail in the publication [3].

3.3.3 Back gradient and back-interface recombination in CIGS absorbers

The highly recombinative CIGS/Mo interface limits the performances of CIGS solar cells. The recombination at the CIGS/Mo interface is influential for the V_{OC} in high-quality CIGS absorbers, especially with an increased diffusion length of charge carriers. A quantitative understanding is needed of the role of the Ga back grading height (ΔGGI) in suppressing back interface recombination. Here, we take advantage of a low-temperature process to modify the ΔGGI by changing Ga and In fluxes in the first stage.

Figure 7(a) shows secondary ion mass spectroscopy (SIMS) depth profiles of selected absorbers fabricated using four different processes. The ΔGGI value was modified over in a wide range: from 0.20 (reference process "R1") to 0.50 (process "O3").

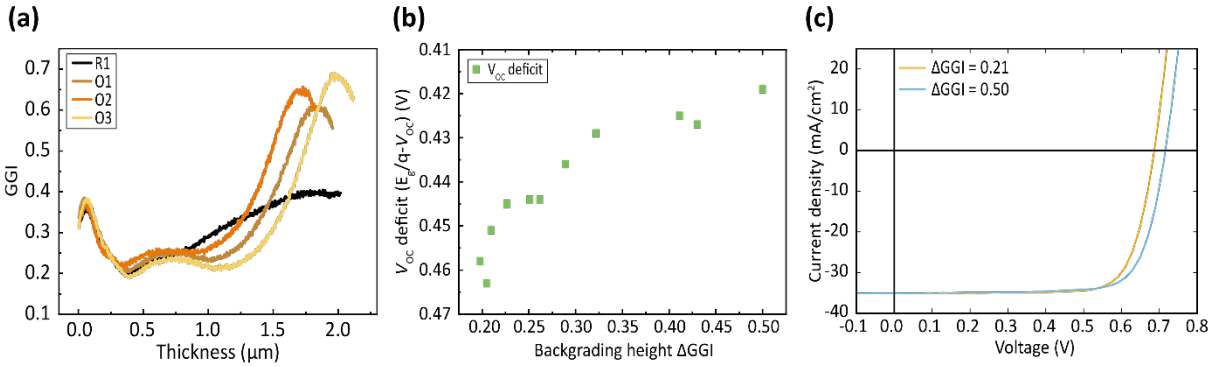

Figure 7: (a) [Ga]/([Ga]+[In]) (GGI) profiles for selected absorbers. (b) V_{OC} of the investigated samples as a function of their ΔGGI values. (c) J-V curves for two selected solar cells with similar bandgap energy and different ΔGGI values.

Figure 7(b) shows the change of V_{OC} values with different ΔGGI. The V_{OC} values improve by about 35 mV when ΔGGI increases from 0.20 to 0.32. An additional V_{OC} gain of 10 mV is obtained with a ΔGGI increase from 0.32 to 0.50. Figure 7(c) compares the current density versus voltage (J-V) curves of two solar cells with similar bandgap energy (Eg) and different ΔGGI (0.21 and 0.50). The sample with a ΔGGI of 0.50 exhibits a strong V_{OC} increase due to higher ΔGGI while the short circuit current (J_{SC}) is comparable for both solar cells, consistent with their similar Eg. Due to the V_{OC} improvement, photovoltaic conversion efficiency (PCE) increases from 18.7% to 19.3%.

As a complementary investigation, we performed TRPL measurements on selected absorbers covering different ΔGGI values. The absorbers with high ΔGGI show considerably longer decay times than the low ΔGGI ones, confirming the reduction in back interface recombination.

3.3.4 Heat-light soaking

CIGS devices have a degree of sensitivity to heat and heat-light soaking (HLS) treatments. This treatment consists in the application of thermal stress on the cell placed under illumination (about 1-sun intensity). In this activity, we investigated the impact of such treatments on CIGS devices deposited on polyimide substrates, notably to reproduce the high doping levels achieved in WP2.

In a first approach, we subjected samples with up to 18 cells to HLS treatments and measured the electrical performances for different time delays after treatment. After stabilization (a few days storage), further HLS treatments were performed with increased thermal stress, as summarized in Figure 8. The device performance increases with additional heat treatment, driven by an increase in V_{OC}. The fill factor and the short circuit current are essentially not affected by the treatments. A slight device degradation was observed after the highest 24h, 120°C treatment. Cell efficiencies above 21% were measured internally after this heat-light soaking treatment.

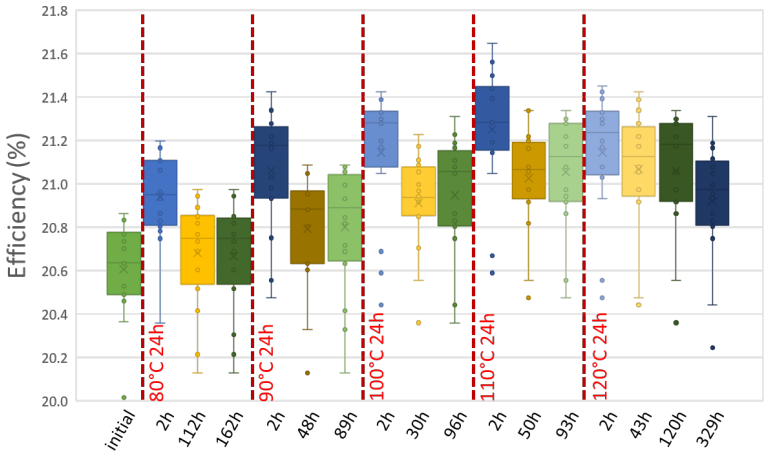

Figure 8: Evolution of device performance after repeated heat-light soaking treatments and relaxation times. The device efficiency increases immediately after heat-light soaking treatment, and the gain partially disappear over time. The higher the HLS temperature, the higher the gain and the long-term cell improvement. The devices start to degrade with HLS treatment at 120°C for 24h.

Building on this initial experiment we performed then a second study with extensive characterization effort. SIMS, temperature-dependent J-V, capacitance versus voltage (C-V), admittance spectroscopy and TRPL characterization were performed to understand the changes in material and electronic properties upon a single heat-light treatment at 110°C on finish device. The performance improvement is long-lasting over the investigated timeframe of several months. We identified changes in the absorber bulk, as well as hints of changes at the interfaces and/or buffer layers. For example, the doping is

strongly increased upon heat-light soaking (see Figure 9b), associated with a moderate increase in alkali concentration in the absorber. Activation energies of capacitance steps are modified, as well as the built-in voltage. The gains related to increased doping are partly offset by a reduction in minority carrier lifetime (Figure 9c) significantly below the radiative limit, which we currently seek to understand and address.

The work allowed to obtain highly-doped absorber layers, similarly as could be achieved in WP2 with steel substrates. We demonstrated a new record CIGS device on a flexible substrate with 21.38% power conversion efficiency (see Table 2). Data analysis is ongoing to gain further insights for a publication. We seek to modify the baseline process to capture the benefits of the HLS soaking treatment while minimizing the corresponding effort and additional processing steps.

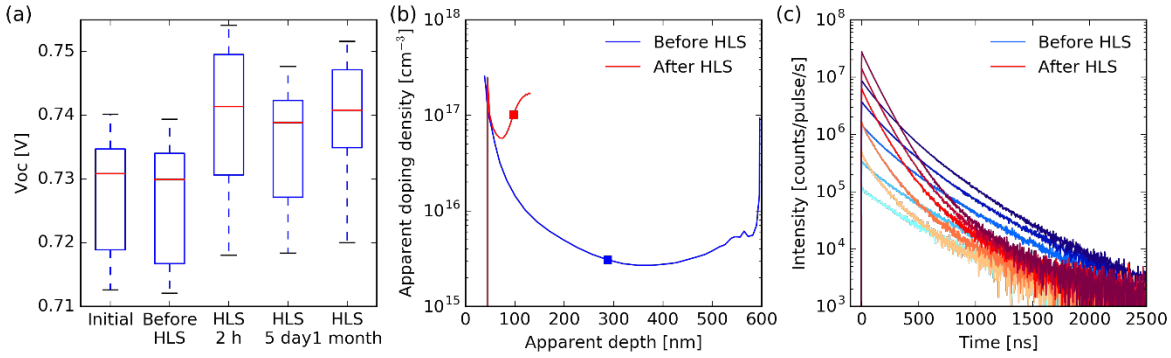

Figure 9: (a) V_{OC} of the cells before HLS, and after various time delays after HLS. The improvement is stable over time. (b) Evaluation of the doping density by capacitance versus voltage measurement. The doping increases by about an order of magnitude after HLS. (c) TRPL signal before and after HLS. The intensity at t=0 increases as per doping level. The gain is partly offset by increased non-recombination lifetime, evidenced by the steeper decays after HLS. The combination of both effects is in agreement with the V_{OC} increase evidenced in (a).

3.3.5 Alloying with silver

Over the course of the project, we identified alloying CIGS with a very small amount of silver as a promising way to improve efficiency and enhance the fabrication process tolerances, which is quite important for robust industrial processing. The ACIGS ((Ag,Cu)(In,Ga)Se_2) material has a lower melting point and grain growth is promoted as compared to usual CIGS. Alloying Ag into CIGS changes its optoelectronic properties by lowering both the conduction and valence band edge and widens the bandgap. The larger grain sizes of ACIGS may lead to fewer structural defects and less sub-bandgap disorder. Therefore, ACIGS appears especially promising for low-temperature processes for example on polyimide substrates, and to widen the tolerances of existing deposition processes.

For our first experiments, we choose an industry-compatible approach where a very thin layer of silver is deposited as a precursor layer on the substrate before absorber deposition. Using this approach, it is in principle possible to upgrade production lines without major modification to the existing equipment. Preliminary experiments yielded good results. We decided to investigate the processing limits towards lower temperature and the robustness of the deposition process, in the perspective of alternative substrates and enlarged process tolerances.

Substrates were prepared with and without a 15 nm silver precursor layer on the Mo-coated glass substrate. CIGS films of about 2.0 µm thickness were deposited at various temperatures on both types of substrates with very similar Cu, In, Ga and Se fluxes. Ag readily alloys into CIGS during deposition, forming ACIGS. Figure 10(left) shows the open-circuit voltage (V_{OC}) for both CIGS and ACIGS solar

cells grown at different substrate temperatures T_{sub}. The maximum 413°C investigated nominal temperature is compatible with flexible polyimide substrates and would yield very similar performances on such substrates. Compared to CIGS, ACIGS benefits from an improved V_{OC} at low deposition temperatures. Efficiencies above 18% could be achieved with a nominal deposition temperature as low as 303°C. A significant drop was only observed with 253°C nominal substrate temperature. On the contrary, the efficiency of CIGS solar cells drops already with 303°C, mainly stemming from a reduced V_{OC}. Lower process temperatures disturb the deposition process and no Ag-free device could be synthesized with 253°C nominal substrate temperature.

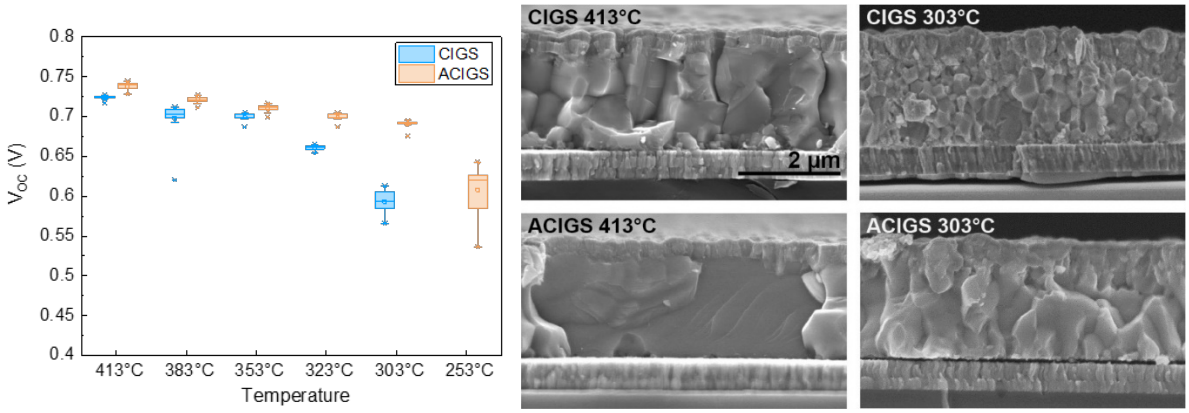

Figure 10: (Left) Open-circuit voltage for ACIGS and CIGS solar cells with absorbers deposited at different nominal substrate temperatures. (Right) SEM cross-sectional images for ACIGS and CIGS at different growth temperatures, showing improved absorber morphology in presence of Ag.

Figure 10(right) shows the morphology differences between ACIGS and CIGS absorbers deposited at low temperatures. The grain size of ACIGS is larger than that of CIGS for both 413°C and 303°C. ACIGS absorbers also exhibit large grains throughout the depth down to the back contact, in contrast to CIGS which exhibits the typical small grain size. Further deterioration in the microstructure is observed for CIGS grown at 303°C. The grain size is very small, resulting in a higher density of grain boundaries and presumably, a higher defect density as grain boundaries (esp. randomly oriented ones) are possible locations for non-radiative recombination traps. The deteriorated morphology is correlated with a significant V_{OC} reduction. Instead, the same growth temperature for ACIGS leads to only a slight deterioration in the microstructure. The alloying with Ag facilitates the Cu diffusion during the deposition process. This finding is especially interesting in the context of fast, high-throughput depositions typical of industrial processes.

This electrical and morphological analysis was completed with additional material and optoelectronic characterization. Admittance, TRPL and X-ray diffraction (XRD) techniques delivered interesting insights. The doping level in the absorbers is comparable in ACIGS and CIGS layers deposited for the highest investigated temperatures. We observe a large reduction in absorber doping concentration below the same temperature for which the V_{OC} is strongly degraded. The non-radiative recombination lifetimes degrade more progressively with decrease substrate temperatures. In addition, XRD measurements revealed that Ag alloying significantly reduces the compressive stress. This reinforces the interest for ACIGS especially for flexible PV applications, for which layer stress can lead to adhesion and delamination issues.

In summary, alloying with silver results in a large improvement of the morphology of the layers, enable absorber deposition at low temperature with widened process tolerances, and lowers the stress in the layers. The alloyed absorbers show improved performances. The precursor approach is compatible with existing co-evaporation hardware. However, questions crucial for industrial implementation remain

open, notably the best strategy for Ag incorporation (we investigated only the precursor layer method and not the co-evaporation), the amounts, and the impacts on the other aspects of the deposition process such as alkali treatments, doping control or process monitoring.

3.3.6 Opportunities for an efficiency boost of next generation CIGS solar cells

As part of the synergies developed within our group and specifically with the EU project HyMet (Hybrid metrology for thin films in energy applications, EMPIR EURAMET), we conducted an analysis of the efficiency losses and prospects for the next efficiency boost for the CIGS photovoltaic technology. The study was published in reference [4]. Specifically, we suggest that devices with non-graded absorbers, integrating charge selective contacts and maximizing photon recycling can lead to efficiencies of 29% under the AM1.5 global spectrum.

3.3.7 Flexible mini-modules

An objective of the project was to assess that the improvements of lab-scale processes can be applied to module making, and ultimately transferrable to module manufacturers. Among the possible PV performance loss mechanisms, we find, (a) optical losses due to thicker transparent conductive oxide (TCO), (b) fill factor (FF) losses due to non-ideal interconnects, (c) V_{OC} losses due to absorber non-uniformities and parasitic shunt paths. A degree of losses is unavoidable, partly due to contradicting requirements in characteristics of high-efficiency modules. Our objective is to limit these cell-to-module losses to improve the performance of mini-module and check that the improved lab process can be applied at larger scale.

a) Mitigation of parasitic optical absorption: laboratory cells are typically fabricated with very thin TCO layers TCO (about 100 Ω/sq) and metal grids as front contact, to reduce the optical parasitic absorption in the TCO. Contrarily, PV modules require a low sheet resistance TCO (about 10 Ω/sq or below) to achieve lateral current transport to the next interconnected solar cells. We first investigated a thick layer of standard Al:ZnO TCO with low carrier mobility. However, the high current loss (> 2 mA/cm^2) due to the increased parasitic absorption made it impossible to achieve high-efficiency PV modules. In a second approach, we replaced most of the Al:ZnO (μHall = 18 cm2V^{-1}s^{-1}) by a high-mobility InZnO (μHall = 47 cm^{2}V^{-1}s^{-1}). However, InO-based compounds can create a Schottky barrier with ZnO because of the difference in carrier concentrations in the layers [5], which reduces the FF. An optimized bilayer stack based on a thin low-doped Al:ZnO layer and a thick InZnO layer was used to optimize the trade-off between electrical transport, band alignment, and optical absorption losses while maintaining the 10 Ω/sq requirement for the TCO sheet resistance. The use of a unique InZnO layer is possible but requires optimization steps, which could not be performed within the last months of the project in 2020.

b) FF losses due to non-ideal interconnects: Figure 11(a) shows a schematic representation of the monolithic cell interconnection. Ideal P1 and P3 are perfectly insulating and P2 perfectly conductive. Non-negligible parasitic resistive or conductive paths appear in real PV modules.

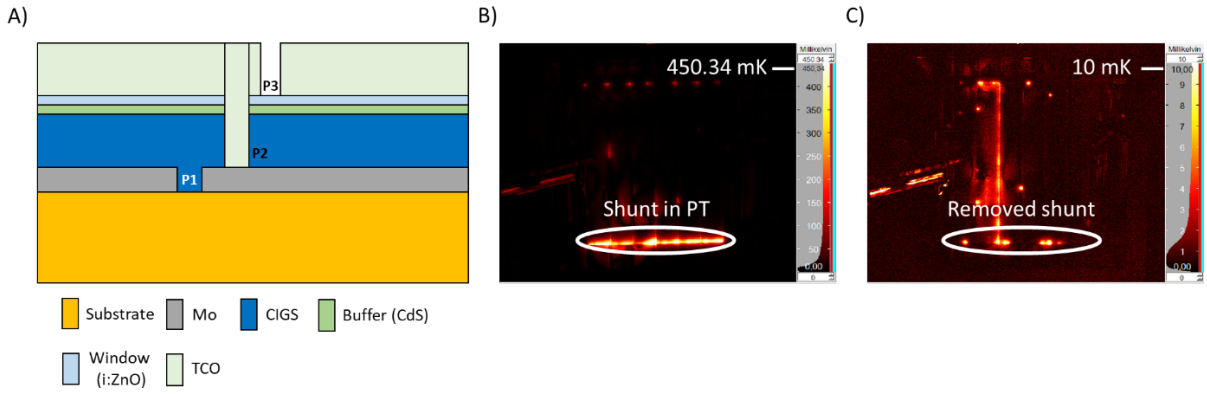

Figure 11: A) Schematic representation of the monolithic interconnection process. B) Thermography image of module shunted along a PT scribe. C) Thermography image of PV module after deposition of alumina, depicting the removed parasitic shunt in PT scribe (note the different temperature scales for the two thermography images).

- The P1 scribe insulates the bottom contact from adjacent cells. The optimal P1 scribe parameters vary depending on the CIGS materials properties, and specifically on the Cu content. For example, a narrow P1 scribe (50 µm) is required for a low Cu content CIGS (e.g. Empa baseline at the start of the project, with CGI = 0.88). As efficiencies increase with modified absorber compositions, the CIGS conductivity increased, and a wider P1 line is now required. However, this reduces the geometrical fill factor and the active area, and, hence, the overall module efficiency. We investigated different P1 widths to insulate the bottom contacts while maintaining the geometrical FF as high as possible. The optimal P1 width for our current CIGS baseline (with high Cu content CGI = 0.98) was found to be 120 µm.
- The P2 conductive scribe connects the top contact to the bottom contact of the adjacent cell. The P2 process was optimized in terms of laser power and TCO deposition parameters to increase the conductivity and minimize the scribe width. We obtained the optimal process with a dual deposition process and a single scribe step where the first thin TCO layer is deposited followed by the P2 scribing step, finalized by deposition of a thick TCO. The optimal P2 scribe resulted in a width of 70 µm and yielded a resistance of 2.1 Ω for 1 mm of scribe length. The specifics of the P2 process and the achievable width are dependent on the laser patterning equipment.
- The P3 insulation scribe removes the TCO between adjacent cells. We evaluated different processes to maximize the resistance of the P3 scribe. Since TCOs are almost transparent at infrared wavelengths, a 1064 nm wavelength laser typically removes the TCO by ablating a thin top underlying CIGS surface layer. However, this process can damage the CIGS surface, form parasitic shunt paths and reduce the module Rp and FF. We investigated P3 scribing with a 355 nm laser instead of a 1064 nm one. In contrast to infrared lasers, UV lasers depose a high percentage of power (≈78 %) in the TCO layer itself instead of in the underlying layer, which prevents laser damage on the CIGS surface and mitigates the formation of parasitic shunt paths.
- PT (module edge definition): The final PT scribe delimits the sides of the module. This is a standard and straightforward process in the industry and is not critical for large-area devices. We can also perform this step without difficulty with layers produced by industrial partners. However, technical issues specific to our absorber thickness and patterning hard-

ware prevented using the usual PT process. We investigated alternative processes for module delimitation. PT from the front was found detrimental to the module performance as it creates parasitic shunt paths between the front and back contact of each cell (see Figure 11(B)). For this reason, we added a series of post-processing steps to the fabrication sequence to prevent the formation or cure the parasitic shunt paths. These steps include the lateral module definition with an extra P3 scribe parallel to the PT scribe line, as well as an AlOx atomic layer deposition (ALD) deposition process to chemically reduce the damaged CIGS surface and to prevent degradation of the lateral scribes by environmental O_2.

c) V_{OC} losses due to absorber non-uniformities and parasitic shunt paths may arise from non-uniformities in the absorber and buffer layers, as well as from plasma damage at the window/TCO interface. Unfortunately, absorber and buffer non-uniformities are very challenging to optimize due to their process-to-process variations in laboratory-scale equipment. We could reduce the plasma damage during TCO deposition by developing an "in steps" deposition method where plasma power is raised slowly during the sputtering process to prevent excessive damage to the window/TCO interface. Furthermore, the optimization of the P1, P3, and PT scribes described above allowed us to achieve a cell-to-module V_{OC} loss of 20mV/cell.

The different points described above were implemented to fabricate a PV mini-module on flexible polyimide. The process flow is presented in Figure 12(A). As compared to standard industrial process, the main differences relate to the 2-step TCO deposition and the conformal coating by chemical vapor deposition (CVD) method. As detailed above, the 2-step deposition was introduced to limit the parasitic absorption losses induced by the use of AZO. It is possible to realize interconnections with a high-performance TCO deposited in a single deposition step, but could not be realized within the timeframe of the project. The edge passivation and protection are very important for our small-size mini-module but experimental issues encountered are very specific to our in-house absorbers. Our findings suggest that passivation and protection may be achieved with a simpler approach, e.g. with a suitable treatment immediately before standard device encapsulation.

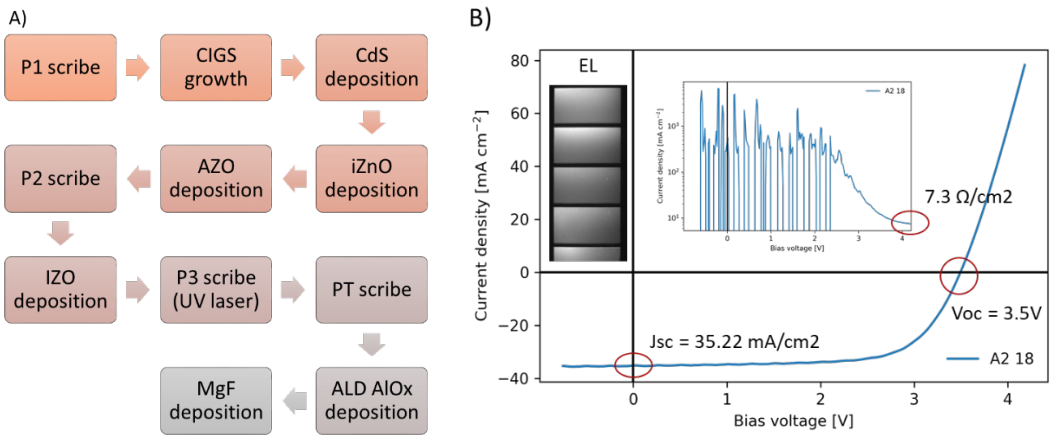

Figure 12: A) Flexible mini-module fabrication process. The relevant differences with industrial processes are the 2-step TCO deposition for optimal management of optics and contacting, and the deposition of a conformal protective coating (AlOx) by CVD method. B) Best performing flexible mini-module fabricated on flexible PI film.

As depicted in Figure 12(B), the best PV parameters were obtained with a 5-cells mini-module as follow: V_{OC} = 3.5 V, J_{SC} = 35.22 mA/cm2, FF = 68.5%, PCE = 16.9%. The electroluminescence image is very uniform, evidencing the good process uniformity of the layers. The average cell performance of the reference device is only 19.0%, corresponding to a cell-to-module loss of 2.1%. This 2.1% cell-to-module

is a good value and is a success in itself. The largest sources of performance degradation are identified, and mitigating measures could be developed. The project proposal specifies 22% cell and 18% mini-module efficiencies, corresponding to 4% cell-to-module losses. We are confident that the 18% mini-module efficiency target is within reach, especially considering the high-efficiency layers demonstrated in Section 3.3.4.

3.3.8 Summary of deliverables and milestones

M1.1: Identify the most suitable glass (with or without buffer) which reproducible delivers more than 20% cells processed at high temperature (12 month)	Reached. A suitable glass was identified. Process temperatures could be increased by about 40°C as compared to regular soda-lime glass.
M1.2: Prove what properties of CIGS grown at high temperature (>550 °C) are different from low temperature grown layers.	Reached. Several key differences in material properties and growth mechanisms were identified (see sections 3.1.3 and 3.2.2)
D1.1: 21% efficiency solar cell (24 month)	Reached. See section 3.1.3.
D1.2: 22% efficiency solar cells with report on what limits the efficiency.	Demonstrated a device with 21.5% efficiency (internal value). Increase in efficiency is about 1% as compared to polyimide substrate. The device limitations are detailed in section 3.1.3 as well as in a publication in preparation.
M2.1: Identification of metal foil to deliver 21% cells (18 month)	Reached. Metal foil with potential to deliver > 21% identified.
M2.2: Benchmarking of processes for 22% cells on metal and effects of deposition temp identified for possible adaptation on polymer at low temperature (30 month)	Achieved 20.15% certified efficiency. The previous internal record was 18%, the world record is 20.5%. Extremely low V_{OC} deficit (indicative of good quality absorber material suitable for high efficiency device) could be achieved. Also, very high doping level that is still under investigations. Currently, performance is limited by FF. Positive outcome for activity on flexible tandem 2-junction devices due to the better suited bandgap. Identified and essentially addressed the critical influence of diffusion barrier on cell performances.
D2.1: 21% solar cells on metal foils (18 month)	See M2.2.
D2.2: 22% solar cells on metal foils (30 month)	See M2.2.
M3.1: conclusion on the effectiveness of UV flash annealing of CIGS for improvement of the properties of CIGS (18 month)	Reached conclusion (Section 3.3.1) The UV flash annealing was assessed and found not effective at improving the cell efficiencies.
M3.2: 21% flexible cell on polymer and identification of what is limiting the efficiency beyond 21% (30 month)	Reached.

M3.3: 22% flexible cell on polymer and identification of what is limiting the efficiency (40 month)	Demonstrated a 21.4% cell (externally certified) This value is a new world record efficiency for flexible CIGS solar cells, and it proves a considerable progress from the 20.4% record value at the start of the project. The limitations of the device are summarized above, as well as in a publication currently in preparation.
D3.1: 21% flexible cell and 17% mini-module on polymer film (30 month)	Reached 21.4% flexible cell (see M3.2) As of M30, work on mini-modules ongoing. Progresses delayed by interruption of lab activity. Processes for module scribing must be adapted in the case of higher-performing absorbers.
D3.2: 22% flexible cell and 18% mini-module on polymer film (40 month)	A 21.4% efficiency cell was externally certified. (See M3.3). We are confident for further enhancement in efficiency based on the knowledge gained in this project. Best mini-module: 16.9%, with only 2.1% cell to module efficiency loss. We are confident that the target is within reach, especially with the improved devices recently demonstrated.

Table 1: Summary table of deliverables and milestones

4 Conclusions

During the ImproCIS project, we demonstrated two new externally certified record efficiencies for CIGS on flexible substrates. As detailed in Table 2, we improved our previous mark in 2019, and again in 2021 with a device with about 21.4% externally certified power conversion efficiency. The improvements result from a combination of modifications of the deposition process and post-fabrication treatments. In addition to the improved record devices, we could also improve the efficiency baseline that provides a stable and reproducible basis for future works.

	Voc [mV]	Jsc [mAcm-2]	FF [%]	Efficiency [%]
Record by start of the project	736	35.1	78.9	20.4
Record 2019 [3]	734.4	36.74	77.17	20.82
Record 2021	746.7	37.35	76.66	21.38

Table 2: Externally certified record power conversion efficiency for CIGS solar cells on flexible substrates. Are reported the record value at the start of the project, and the new values demonstrated during the extent of the project.

The nature of the substrate plays a marginal role for low-temperature processes (~450°C compatible with polyimide substrates). The properties of the layers deviate with processing at higher temperatures. Steel substrates affect the formation of the bandgap gradient and lead to a strong increase in doping. But, the reduced mobility and diffusion length warn of possible fundamental issues with the high-temperature steel route. CIGS layers are improved with high-temperature processing on glass, yielding about 1% absolute efficiency gain. The improvement of high-temperature processes increases V_{OC} due to reduced density of defects and non-radiative recombination. While the low process temperatures imposed by the use of polyimide substrates slightly degrade the device performances, we identified no roadblock towards further efficiency progresses.

A promising path for further efficiency progresses is the addition of a small amount of Ag in the layers. Our initial experiments on glass substrates show improvements in the absorber morphologies and suggest possibilities for significant efficiency gains, especially with low-temperature processes. We demonstrated that the parameter window for deposition temperature is significantly enlarged. Adaptation of the acquired knowledge should enable enhancement in deposition rate of good quality absorber layers. Fast and robust deposition processes are highly desirable for increasing the production throughput on an industrial scale. However, future research is needed to prove the hypothesis, especially for flexible solar cells on polyimide film.

We also investigated limitations to the performances of current devices and strategies to go beyond these limitations. We clarified the requirements on GGI gradient in high-performance absorbers and quantified the performance losses when these requirements are not met. We also evaluated the potential of the CIGS technology based on current state-of-the-art devices, irrespective of process specifics, and therefore of general interest for the community of CIGS research groups and manufacturers.

A cell-to-module efficiency loss of 2.1% was achieved with a mini-module on flexible PI film, which yielded a PCE = 16.9%. This 2.1% cell-to-module loss is within expectations of good module-making processes, while industrial modules may have 2 to 3 times higher loss. We systematically investigated the contributors to efficiency loss and could reduce the optical and electrical losses. Optimization aspects include mitigation of optical losses in the high conductance TCO and the reduction of resistive losses at scribe lines by switching the conventional 1064 nm laser for a 355 nm laser. We developed TCO deposition recipes to mitigate the plasma damage. Further improvements are identified to mitigate the remaining FF losses. The difficulties encountered with PT scribe are essentially irrelevant for large-sized industrial modules. We are confident that the 18% mini-module efficiency target is within reach, especially considering the high-efficiency layers demonstrated in section 3.3.4.

5 Outlook and next steps

Thanks to the ImproCIS project we improved the efficiency of our solar cells on polyimide substrates, for both record and baseline devices. In this context, the new record value of 21.4% is proof of advancement in the state of the art of flexible CIGS solar cell.

A research direction is to better understand the effect of heat-light soaking treatment at the material level, to obtain the same effects on device properties as part of the regular fabrication process.

We have identified a very promising pathway for the next efficiency gains by adding a very small amount of Ag in the form of a precursor layer, which is compatible with industrial implementation. We demonstrated the possibilities of device quality ACIGS at very low temperatures on glass substrates. However, we did not use Ag in our high-efficiency processing line and also not yet on polyimide film substrates, but we are confident of further efficiency improvements of flexible solar cells and the possibility of high growth rate deposition of absorber layers. We also want to investigate different strategies for Ag incorporation (precursor layer or different possibilities with co-evaporation), to identify the optimal method in view of high device efficiency and robust manufacturability. This work, if developed further, will be very useful for roll-to-roll manufacturing of solar modules with enhanced growth rate.

The efficiency targets for mini-modules could not be reached. We experienced some issues, notably with the improved absorber layers as well as with the processing hardware. The project suggests the importance of a regular reassessment of the impact on the manufacturability of the process changes in high-efficiency laboratory processes. Nevertheless, we could solve or mitigate the sources of cell-to-module efficiency losses, demonstrating a low 2.1% cell-to-module efficiency loss. We are confident that the 18% efficiency target is within reach, especially considering the excellent progress achieved with solar cells. We emphasize that the interconnection processing must be continuously adapted to the evolving absorber state-of-the-art. Currently, industrially produced modules have a large gap in efficiency from small single cells. Besides the losses related to the larger area, shunting and scribing-related interconnection losses are significant contributors to the efficiency gap. Our work provides some insights into possibilities to reduce those cell-to-module losses in industrial modules.

6 Publications

The following peer-reviewed publications were published as of April 2021.

1. Yang S.-C., Ochoa, M., Hertwig, R., Aribia, A., Tiwari, A. N., Carron, R. (2021). Investigation of back grading influence on voltage loss in low-temperature co-evaporated Cu(In,Ga)Se2 solar cells. Prog Photovolt Res Appl. 2021;1–8. https://doi.org/10.1002/pip.3413
2. Yang, S.-C., Sastre J., Krause, M., Sun, X., Hertwig, R., Ochoa, M., Tiwari, A. N., Carron, R. (2021). Silver-Promoted High-Performance (Ag,Cu)(In,Ga)Se2 Thin-Film Solar Cells Grown at Very Low Temperature. Sol. RRL 2021, 2100108. https://doi.org/10.1002/solr.202100108
3. Ramis Hertwig, Shiro Nishiwaki, Mario Ochoa, Shih-Chi Yang, Thomas Feurer, Evgeniia Gilshtein, Ayodhya N. Tiwari and Romain Carron. ALD-ZnMgO and absorber surface modifications to substitute CdS buffer layers in co-evaporated CIGSe solar cells. EPJ Photovolt., Volume 11, 12, 2020, Chalcogenide Materials for Photovoltaics 2020. https://doi.org/10.1051/epjpv/2020010
4. Ochoa, M., Buecheler, S., Tiwari, A. N., & Carron, R. (2020). Challenges and opportunities for an efficiency boost of next generation Cu(In,Ga)Se2 solar cells: prospects for a paradigm shift. Energy and Environmental Science, 13(7), 2047 (9 pp.). https://doi.org/10.1039/D0EE00834F
5. Carron, R., Nishiwaki, S., Feurer, T., Hertwig, R., Avancini, E., Löckinger, J., … Tiwari, A. N. (2019). Advanced alkali treatments for high-efficiency Cu(In,Ga)Se2 solar cells on flexible substrates. Advanced Energy Materials, 9(24), 1900408 (8 pp.). https://doi.org/10.1002/aenm.201900408
6. Feurer, T., Carron, R., Torres Sevilla, G., Fu, F., Pisoni, S., Romanyuk, Y. E., … Tiwari, A. N. (2019). Efficiency improvement of near-stoichiometric CuInSe2Solar cells for application in tandem devices. Advanced Energy Materials, 9(35), 1901428 (6 pp.). https://doi.org/10.1002/aenm.201901428
7. Carron, R., Andres, C., Avancini, E., Feurer, T., Nishiwaki, S., Pisoni, S., … Tiwari, A. N. (2019). Bandgap of thin film solar cell absorbers: a comparison of various determination methods. Thin Solid Films, 669, 482-486. https://doi.org/10.1016/j.tsf.2018.11.017

In addition to the publications already available, several manuscripts were submitted or are in preparation on the following topics.

8. Charge carrier dynamics and performance evaluation of Cu(In,Ga)Se2 solar cells by means of Time-Resolved-Photoluminescence microscopy (in preparation)
9. Lateral charge carrier transport in Cu(In,Ga)Se2 by use of time-resolved photoluminescence mapping (in preparation)
10. Impact of heat-light soaking on device characteristics and performances of CIGS solar cells (in preparation)

7 References

List of cited references

[1] Yang, S., Sastre, J., Krause, M., Sun, X., Hertwig, R., Ochoa, M., Tiwari, A.N. and Carron, R. (2021), Silver-Promoted High-Performance (Ag,Cu)(In,Ga)Se2 Thin-Film Solar Cells Grown at Very Low Temperature. Sol. RRL 2100108. https://doi.org/10.1002/solr.202100108

[2] http://miasole.com/miasole-achieves-flexible-substrate-thin-film-solar-cell-efficiency-of-20-56-percent

[3] Carron, R., Nishiwaki, S., Feurer, T., Hertwig, R., Avancini, E., Löckinger, J., … Tiwari, A. N. (2019). Advanced alkali treatments for high-efficiency Cu(In,Ga)Se2 solar cells on flexible substrates. Advanced Energy Materials, 9(24), 1900408 (8 pp.). https://doi.org/10.1002/aenm.201900408

[4] Ochoa, Mario, Stephan Buecheler, Ayodhya N. Tiwari, and Romain Carron. 2020. “Challenges and Opportunities for an Efficiency Boost of next Generation Cu(In,Ga)Se 2 Solar Cells: Prospects for a Paradigm Shift.” Energy & Environmental Science 13(7): 2047–55. http://xlink.rsc.org/?DOI=D0EE00834F (August 30, 2020).

[5] Rau, U. and Schock, H. W. 1999. Appl. Phys., 69: 131–147